An unexpected one-pot synthesis of 7-isopropyl-3,3-dimethyl-10'*H*-spiro(indoline-2,9'-phenanthren)-10'-one

Lidong Li,[a] Clara S. B. Gomes,[a] Pedro T. Gomes,[a]* Luís F. Veiros,[a] and Sang Youl Kim[b]

[a]*Centro de Química Estrutural, Departamento de Engenharia Química e Biológica, Instituto Superior Técnico, Av. Rovisco Pais, 1049-001 Lisboa, Portugal*
[b]*Department of Chemistry and School of Molecular Science (BK21), Korea Advanced Institute of Science and Technology (KAIST), 371-1, Guseong-Dong, Yuseong-Gu, Daejeon 305-701, Republic of Korea*
E-mail: pedro.t.gomes@ist.utl.pt

Abstract
The reaction of two commercially available compounds, phenanthrenequinone and 2,6-dialkylaniline (alkyl = Me, *i*Pr), catalyzed by formic acid, in refluxing methanol, gave rise exclusively to 10-(2,6-dialkyl-phenylimino)-10*H*-phenanthren-9-one compounds (alkyl = Me (**1**), *i*Pr (**2**)). In refluxing toluene, and when diisopropylaniline is employed, the heterocyclic compound 7-isopropyl-3,3-dimethyl-10'*H*-spiro(indoline-2,9'-phenanthren)-10'-one (**3**) was unexpectedly prepared as the major reaction product, in the presence of catalytic amounts of various Brønsted acids. DFT calculations indicate that the conversion of **2** into **3** involves a sigmatropic rearrangement as rate limiting step with a high energy barrier (25-28 kcal/mol), in agreement with the requirement of high reaction temperatures.

Keywords: Amination, cyclization, density functional calculations, N,O ligands, phenanthrenequinone

Introduction

In the last two decades, the use of catalysts based on late-transition metal complexes containing Schiff base ligands opened a new era in the development of olefin addition polymerization.[1] The seminal work of Brookhart and coworkers in the preparation of neutral and cationic Ni(II)- or Pd(II)-based complexes containing α-diimine ligands (I and II) led to highly active ethylene propylene or α-olefin polymerization catalytic systems for the production of polyolefins with good microstructural selectivities, such as branched polymers with controllable topological

structures.[2] The control of the selectivity in these catalysts is based on the versatile nature of these ligands, whose arylimino groups are easily modified, allowing different electronic and steric environments of the final complexes. Likewise, Brookhart and Gibson groups discovered that 2,6-diiminepyridines (**III**) are suitable ligands for the preparation of neutral or cationic Fe(II)-, Fe(III)- or Co(II)-based complexes, which are able to polymerize ethylene or propylene with high activities, producing linear oligomers or polymers.[3]

Tremendous efforts have been devoted to design novel late-transition complexes based on Schiff bases and to extend their applications in academia or in industry.[4] It is noteworthy that more recently a kind of neutral nickel complexes based on salicylaldimine (**IV**) and anilinotropone (**V**) have been reported by Grubbs and Brookhart groups, respectively, which are more tolerant towards functional groups when compared to cationic nickel complexes, and are able to catalyze olefin polymerization in emulsion or water media.[5]

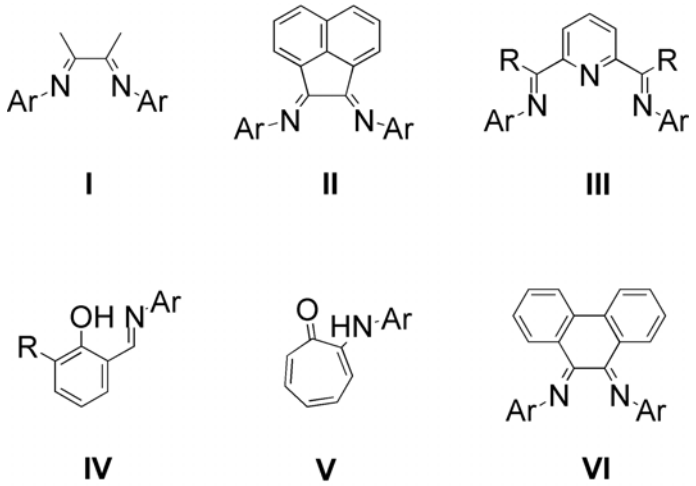

Following these findings, we set out to prepare Ni(II) or Pd(II) complexes containing the α-diimine ligand **VI**,[6] which has substantial structural similarities with **II**. However, we found out that ligand **VI** can not be formed by dehydrating condensation of phenanthrenequinone and 2,6-dialkylaniline, in the presence of common Brønsted acids as catalysts, *e.g.* HCOOH, H_2SO_4, HCl, etc. Surprisingly, the new compound 7-isopropyl-3,3-dimethyl-10'*H*-spiro(indoline-2,9'-phenanthren)-10'-one (**3**) was prepared in a one-pot reaction as phenanthrenequinone reacted with 2,6-diisopropylaniline. Herein, we describe this specific reductive spirocyclization reaction and investigate its mechanism by DFT calculations.[7]

Results and Discussion

In order to synthesize the α-diimine ligand **VI** based on phenanthrenequinone, we have investigated reactions of the latter compound with substituted anilines under diverse conditions. Among them, the dehydrating condensation of a ketone and an aniline in the presence of acids is

known to be one of most efficient processes for preparing this kind of Schiff bases.[8] As displayed in Scheme 1, the condensation reaction successfully occurs in methanol, in the presence of formic acid, but the monoimines **1** and **2** are exclusively formed, in yields of 58 and 42%, respectively, by virtue of a high steric hindrance, even if more than two equivalents of substituted anilines are used, which is consistent with the discoveries of Kocherova *et al.*[9] and Elsevier *et al.*[6] The latter authors prepared a series of α-diimine compounds, 9,10-bis(arylimino)-9,10-dihydrophenanthrenes (where aryl is phenyl or *o*-monosubstituted phenyl), by reductive alkali-metal-mediated cyclodehydrogenation of α,α'-bis(arylimino)bibenzyls and disclosed that the increased steric demands of the arylimine moiety dramatically hamper the ring closure by preventing its occurrence.

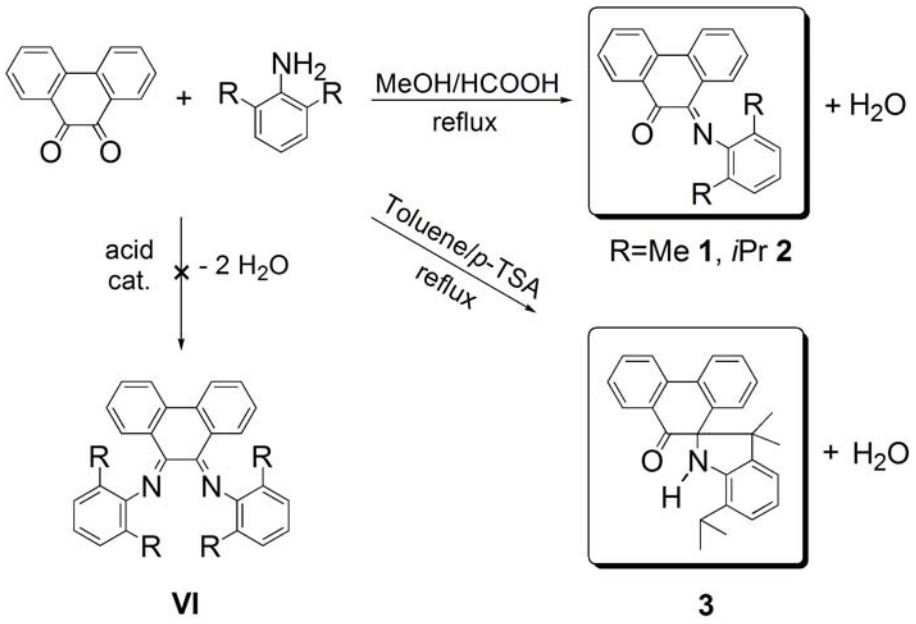

Scheme 1

We have found that the use of more severe conditions was required for the sake of circumventing steric hindrance. Reaction temperatures of *ca.* 140 °C were employed with continuous removal of the water formed in the reaction by a Dean-Stark trap, the methanol/formic acid system being replaced by toluene/*p*-toluenesulfonic acid (TSA). An unexpected reductive amination and alkylation coupling product (**3**) was eventually produced, in yields of 20-42%, accompanied by a small amount of **2** (<15%), as phenanthrenequinone reacted with 2,6-diisopropylaniline, whereas the equivalent reaction did not occur in the case of 2,6-dimethylaniline.

Bright yellow single crystals of **3** suitable for X-ray diffraction characterization were obtained by recrystallization from a diluted heptane solution, and the corresponding molecular structure was determined (Figure 1). Compound **3** crystallized in a monoclinic space group $P2_1/n$. Due to the existence of a chiral centre (C14) in compound **3**, the corresponding

asymmetric unit cell of **3** shows a racemic mixture, composed by two pairs of (*R*)- and (*S*)-enantiomers (see Figure S1 of Supplementary Material). The solid state structure of **3** is compatible with the solution data obtained by ^{1}H and ^{13}C NMR spectroscopies, and also by mass spectrometry (see Figures S2-S10 of Supplementary Material).

The reaction conditions have substantial influence on the course of the reaction (Table 1). Strong acids such as TSA, H_2SO_4 and HCl give **3** in moderate yields and a small amount of **2** as side product, while the relatively much weaker acetic acid produces **3** in lower yield, roughly half of that obtained for **2**. In addition, a concentration of 5 mol % of acid seems to be indispensable to obtain good yields.

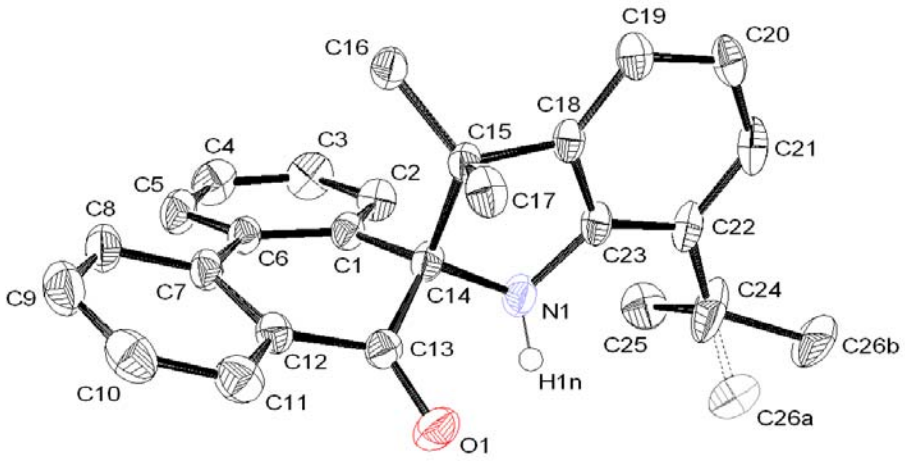

Figure 1. ORTEP diagram of **3** with 50 % probability displacement ellipsoids. Calculated hydrogen atoms have been omitted for clarity. Carbon atom C26 was found to be disordered over two positions. Selected bond distances and angles: C13–O1 1.226(2) Å, C14–N1 1.465(2) Å, C23–N1 1.395(3) Å, C13–C14–C1 108.94(16)°, N1–C14–C15 104.79(15)°, C23–N1–C14 109.90(17)°.

Table 1. The influence of several Brønsted acids on the reaction of phenanthrenequinone with 2,6-diisopropylaniline[a]

Entry	Acids	Yields
1	TSA[b] (2 mol %)	**3** (20 %), **2** (15 %)
2	TSA (5 mol %)	**3** (40 %), **2** (<10 %)
3	TSA (10 mol %)	**3** (42 %), **2** (<10 %)
4	H_2SO_4 (5 mol %)	**3** (44 %), **2** (<10 %)
5	HCl (5 mol %)	**3** (47 %), **2** (<10 %)
6	CH_3COOH (5 mol %)	**3** (12 %), **2** (20 %)

[a] General reaction conditions: 9.60 mmol of 2,6-diisopropylaniline was reacted with 4.80 mmol of phenanthrenequinone, in 50 ml of toluene, at *ca.* 140 ºC, with continuous removal of water by a Dean-Stark trap. [b] TSA refers to *p*-toluenesulfonic acid monohydrate.

In comparison with the monoimine **2**, the secondary amine nature of **3** indicates that its formation from phenanthrenequinone and 2,6-diisopropylaniline involves a reductive amination process. In typical reductive amination reactions of aldehydes or ketones, reducing agents (*e.g.* $NaBH_4$) are generally indispensable and should reduce the imine selectively over its parent aldehyde or ketone.[10] In this work, no additional reducing agents are used, being these reaction conditions similar to those of the Leuckart-Wallach (LW) reductive amination reaction.[11] However, the LW reactions, besides requiring high temperatures (mostly above 180 ^{o}C), are not highly selective, usually giving N-formyl derivatives as the main reaction products, which is not the case observed in the formation of **3**. In addition, it is noteworthy that an alkylation coupling process simultaneously occurs in the reaction. It seems that the tertiary hydrogen belonging to the isopropyl group acts as potential reducing agent towards the imine and, simultaneously, the secondary carbon of the isopropyl group couples with the imine carbon atom.

DFT calculations show that compound **3** is thermodynamically more stable than compound **2** by 16 kcal/mol. However, the methanol/formic acid system gives exclusively compound **2**, while the toluene/*p*-toluenesulfonic acid system gives rise to compound **3**, as the major product, along with a small amount of **2**, as side product. Experimentally, the most prominent difference between these two catalytic systems is their operating reaction temperature, which is basically dictated by the boiling point of each solvent. In fact, the reaction temperature of the toluene/*p*-toluenesulfonic acid system (*ca.* 140 ^{o}C) is much higher than that of methanol/formic acid one (*ca.* 70 ^{o}C), indicating that high reaction temperatures are crucial to promote the conversion of **2** to **3**. According to these results, compound **2** may be regarded as the kinetic product of the process, whereas **3** is the thermodynamic product. In addition, the formation of **3** should be associated with a high energy barrier, justifying the need of high reaction temperatures.

The conclusions discussed above were tested through DFT mechanistic investigations on the conversion of **2** to **3**. In the calculated mechanism, based on a molecule of **2** (Scheme 2), the first step corresponds to a 1,7-sigmatropic rearrangement, yielding **4**. This step is followed by *N*-

protonation, that should be easy to occur under acidic conditions, with the simultaneous formation of a carbocation on the isopropyl tertiary C-atom, yielding **5**. Species **5** undergoes a rapid C–C bond formation producing the protonated ketone **6**, and, finally, deprotonation of the O-atom in **6** yields product **3**.

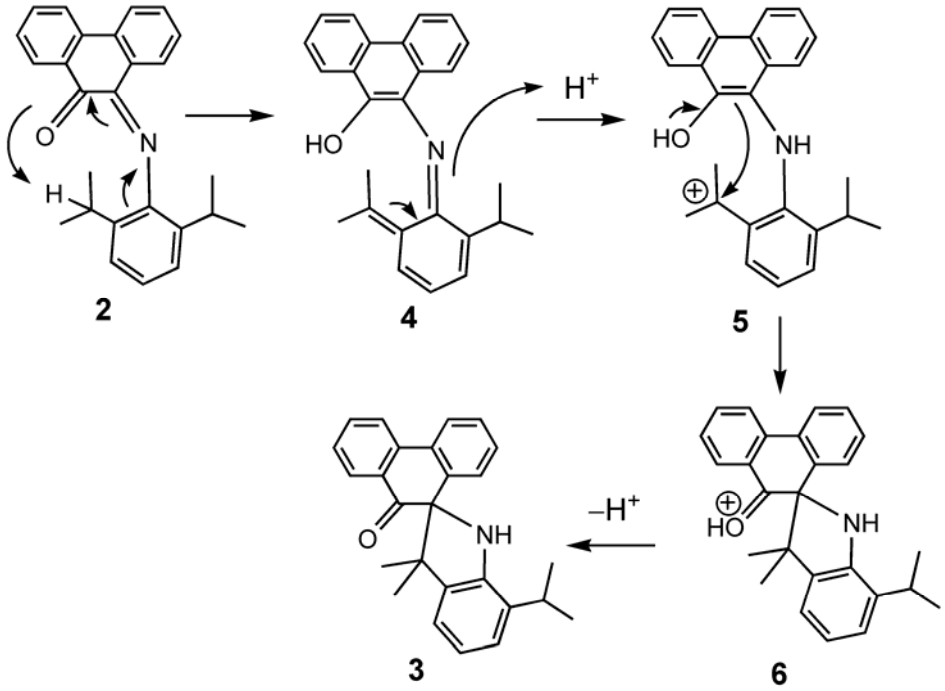

Scheme 2. Mechanism of the conversion of **2** to **3** as studied by DFT.

The proton exchange steps in the mechanism represented in Scheme 2 (from **4** to **5**, and from **6** to **3**) are presumed to occur easily in acidic medium, but are very difficult to simulate from a computational point of view. Thus, the calculations were focused on the first step, the sigmatropic rearrangement from the ketone **2** to the enol **4**, and on the third step, the heterocycle ring closure through C–C bond formation, from **5** to **6**.

The free energy profile calculated for the first step of the mechanism, from **2** to **4**, is presented in Figure 2, with the optimized structure obtained for the species involved. This step corresponds to H-transfer from the carbon atom of the isopropyl group to the O-atom of the ketone in **2**, producing the enol intermediate **4**, in what can be viewed as a 1,7-sigmatropic rearrangement. The corresponding transition state, $\mathbf{TS_{24}}$, is a rather late one, since formation of the new O–H bond is almost accomplished, once $\mathbf{TS_{24}}$ is reached. In fact, both a distance of 1.17 Å and a Wiberg index (WI)[12] of 0.39 are indicative of a very strong O–H interaction, in $\mathbf{TS_{24}}$. This is the rate determining step of the mechanism, with a calculated free activation energy of 25 kcal/mol.

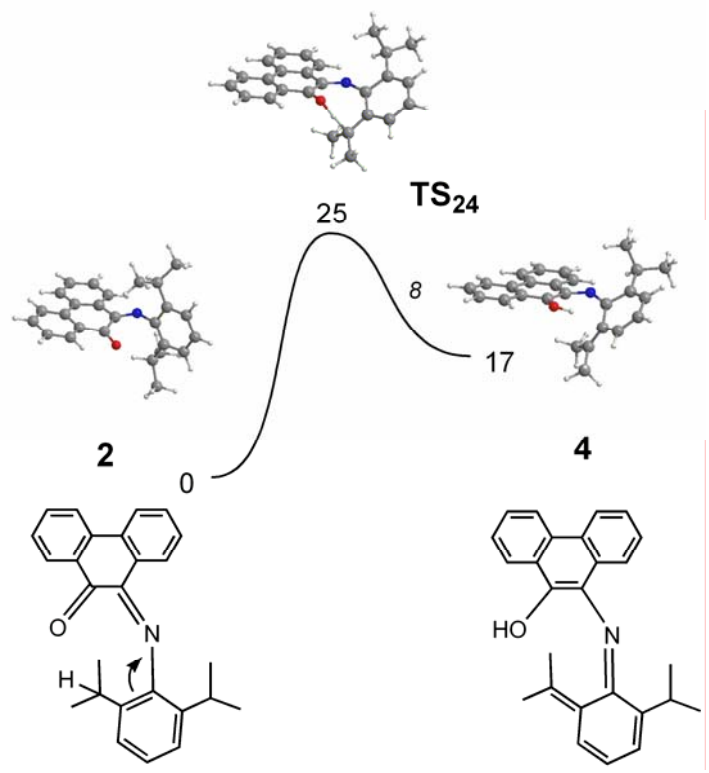

Figure 2. Free energy profile calculated for the conversion of **2** to **4**. The minima and the transition states were optimized and the corresponding structures are represented. The free energy values in kcal/mol, and the free energy barriers are indicated in italics.

In the third step of the mechanism there is the C–C bond formation and closure of the 5-membered heterocyclic ring, from **5** to **6**. The free energy profile calculated for this step is represented in Figure 3, with the optimized structures of the relevant species. In the transition state, $\mathbf{TS_{56}}$, the new C–C bond is only incipient with a very long distance and a Wiberg index indicative of a weak interaction: d_{C-C} = 2.84 Å, WI = 0.05. This makes $\mathbf{TS_{56}}$ an early transition state, similar to the reagent, **5**. The low value calculated for the free activation energy associated with this step (3 kcal/mol) indicates a rather facile process.

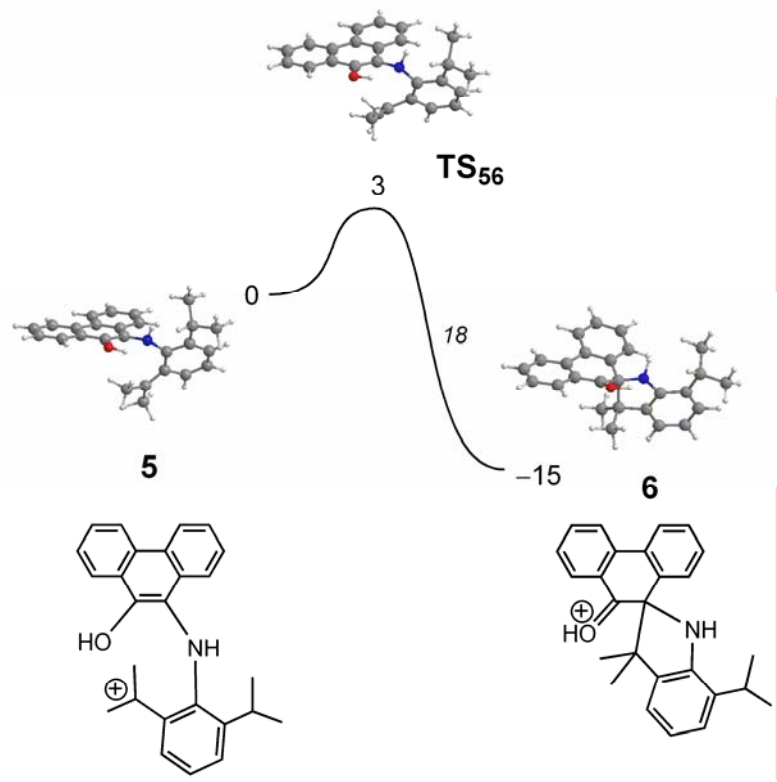

Figure 3. Free energy profile calculated for the conversion of **5** to **6**. The minima and the transition states were optimized and the corresponding structures are represented. The free energy values in kcal/mol, and the free energy barriers indicated in italics.

It is interesting to notice that the intermediate **6** is stabilized by an intramolecular H-bond with the protonated ketone group as H-donor (C=OH) and the N-atom as acceptor. Although this OH···N interaction is presented along the entire step, as shown by the OH···N distances of 2.23 and 2.20 Å in **5** and $\mathbf{TS_{56}}$, respectively, it becomes especially important in **6**, with a OH···N distance of 1.73 Å. The relevance of the intramolecular H-bond in **6** was evaluated through the optimization of a conformer of **6** (denoted **6'**) without that interaction. While in **6** the orientation of the OH group is such that the H atom is pointing toward the nitrogen, in **6'** the OH group is rotated by about 180°, in such a way that the H atom is pointing to the opposite direction of the nitrogen. A comparison between **6'** and **6** reveals that the former is considerably less stable (ΔG = 14 kcal/mol) and gives a semi-quantitative indication on the stabilization of intermediate **6**, due to the intramolecular H-bond.

The mechanistic proposal discussed above was further developed with a study based on a more complete model aiming the simulation of the acidic medium and, particularly, allowing the possibility of an acid catalyzed path. For this, a complete mechanism for the reaction was calculated with the explicit consideration of one acid molecule, modeled by methanesulfonic acid, CH_3SO_3H, for computational expediency. The free energy profile obtained is presented in Figure 4.

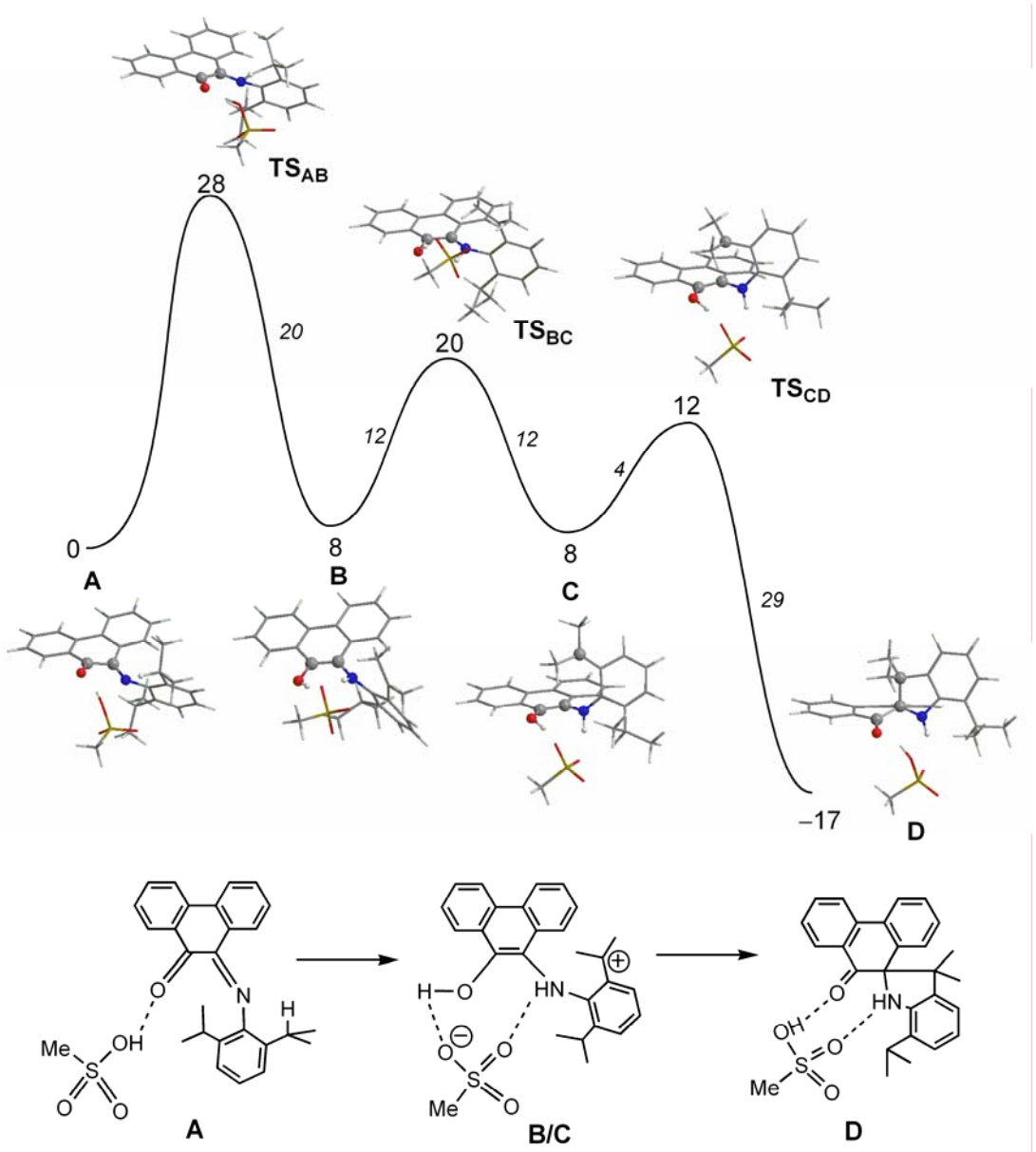

Figure 4. Free energy profile calculated for the conversion of **2** to **3** with an adjacent molecule of methanesulfonic acid. The minima and the transition states were optimized and the corresponding structures are represented. The free energy values (kcal/mol) are referred to the initial reagent (**A**), and the free energy barriers are indicated in italics.

In the mechanism represented in Figure 4, the initial reactant (**A**) corresponds to the monoimine **2**, hydrogen-bonded to the acid molecule ($d_{OH\cdots O}$ = 1.68 Å), while the final product (**D**) is the heterocyclic compound **3**, connected to the molecule of methanesulfonic acid through two H-bonds, using both the OH bond of the acid, and the NH group of the amine: $d_{OH\cdots O}$ = 1.68 Å and $d_{NH\cdots O}$ = 2.00 Å. The calculated mechanism comprises three steps. In the first step, there is simultaneous substrate protonation and H-transfer, from **A** to **B**. This step is equivalent to the

first two steps of the mechanism of the simpler model discussed above (Scheme 2): from **2** to **4**, and from **4** to **5**. In short, the H-transfer process occurring in the first step (from **A** to **B**) is assisted by the neighboring acid molecule through protonation of the O-atom, and, thus, the intermediate **B** is, in fact, an ion pair composed, on one side, by the enol with a formal carbocation located in the isopropyl substituent, and, on the other, by the methanesulfonate anion. The two ions in **B** are strongly connected by two H-bonds: $d_{O\cdots HO}$ = 1.61 Å, and $d_{O\cdots HN}$ = 1.70 Å. In the transition state, $\mathbf{TS_{AB}}$, hydride transfer is well advanced with the C–H bond severely weakened (d = 1.50 Å) and the new N–H bond almost formed (d = 1.20 Å). This is corroborated by the Wiberg indices associated with those bonds, WI_{C-H} = 0.29 and WI_{N-H} = 0.29. At the same time, protonation of the ketone O-atom is only incipient in $\mathbf{TS_{AB}}$, with a still long distance for the new O–H bond (1.50 Å), and a low Wiberg index (0.16), indicative of a weak interaction. This corresponds to the rate limiting step of the mechanism with a rather high activation energy, $\Delta G^{\ddagger}$ = 28 kcal/mol. It is important to notice that this value is similar to the one calculated with the simpler model (within 3 kcal/mol, see above) and both are in good accordance with the requirement of high reaction temperatures, experimentally verified.

The second step of the mechanism, from **B** to **C**, corresponds to a rearrangement around the amine N-atom, bringing the diisopropylphenyl substituent (R) from one side of the molecule to the other. That is accomplished through a rotation around the C–NHR bond, and allows a substrate conformation, in **C**, that is favorable for the C–C bond formation that will occur in the last step. In fact, along this step the two relevant carbon atoms approach, as shown by the corresponding separation: 4.14, 3.85 and 3.14 Å, in **B**, $\mathbf{TS_{BC}}$, and **C**, respectively. The two intermediates, **B** and **C**, are equally stable and the conformational rearrangement has a moderate free energy barrier of 12 kcal/mol.

In the final step of the calculated mechanism, from **C** to **D**, there is formation of a new C–C bond and the consequent closure of a 5-membered cycle. At the same time, the O-atom is deprotonated yielding the ketone group of the product and regenerating the methanesulfonic acid (CH_3SO_3H), both molecules being connected by two H-bonds (in **D**). The transition state for the third step, $\mathbf{TS_{CD}}$, is an early one, as formation of the new C–C is only incipient with a long separation (2.52 Å) and a small Wiberg index (0.16), indicative of a weak interaction, still far from the corresponding values in the product, **D**, where the formation of the C–C is accomplished (d = 1.62 Å, WI = 0.89). Accordingly, the deprotonation of the enol O-atom is only starting in the transition state, $\mathbf{TS_{CD}}$, with a short (1.05 Å) and a strong O–H interaction (WI = 0.49), not far from what is observed in intermediate **C** (d_{O-H} = 1.02 Å, WI = 0.54). This final step is fairly easy, with a free energy barrier of only 4 kcal/mol, and very favorable, with an energy variation of –25 kcal/mol, reflecting the thermodynamic stability of the amine as reaction product.

It should be mentioned that a concerted mechanism (single step) was also explored for the model with explicit consideration of the acid molecule (CH_3SO_3H). The free energy profile obtained for the concerted mechanism is presented in Figure 5. The mechanism obtained starts with **E**, a conformer of **A**, and the path follows a single step with simultaneous C–C bond

formation and H-transfer, assisted by the neighbor acid molecule. In the calculated transition state, $\mathbf{TS_{ED}}$, formation of the new C–C bond is far from accomplished as demonstrated by a long separation (2.99 Å) and a low Wiberg index (0.16). However, the corresponding energy barrier (45 kcal/mol), calculated for such mechanism makes that path not competitive, compared to the ones discussed above.

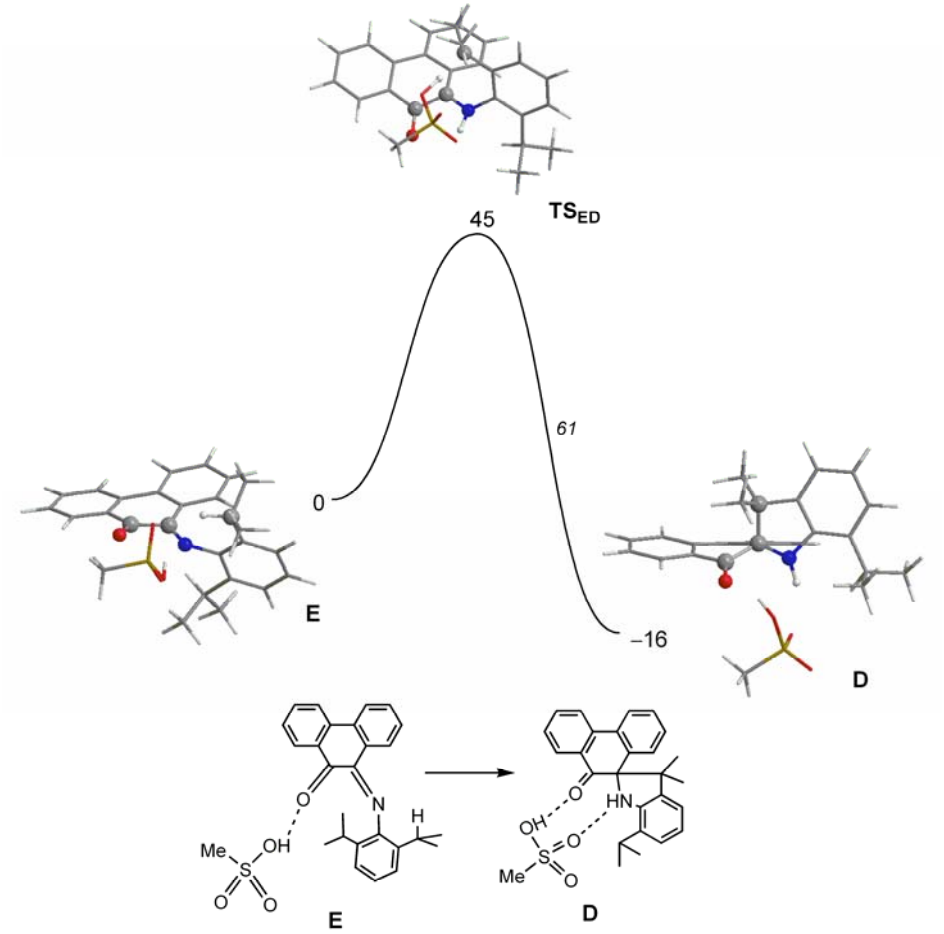

Figure 5. Free energy profile calculated for the direct conversion of **2** into **3** with an adjacent molecule of methanesulfonic acid, through a concerted single-step mechanism. The minima and the transition state were optimized, and the corresponding structures are represented. The free energy values (kcal/mol) are referred to the initial reagent (**E**), and the free energy barriers are indicated in italics.

Interestingly, the absence of the corresponding cyclization reaction in the case of monoimine **1**, can be related to the carbocation nature of the intermediate in the calculated mechanisms above (**5** for the simpler model; **B** and **C** in the more complex one). In fact, in the case of **1**, the arylimine substituents are methyl groups (R = Me), and not *i*Pr as in **2**, which would lead to a less substituted and, consequently, less stable intermediate.

Conclusions

In summary, the acid catalyzed reaction of phenanthrenequinone and excess of 2,6-dialkylaniline (alkyl= Me, iPr) leads, at low temperatures, in refluxing methanol, to the corresponding monoimines **1** and **2** and, on the other side, when 2,6-diisopropylaniline is employed, at higher temperatures, in refluxing toluene, the intramolecular reductive spirocyclization product 7-isopropyl-3,3-dimethyl-10'*H*-spiro(indoline-2,9'-phenanthren)-10'-one (**3**) is obtained as the major product. According to the calculated mechanism, the reaction starts with an acid-catalyzed sigmatropic rearrangement as the rate limiting step, being followed by a rapid C–C bond formation, yielding the final product **3**, which contains a 5-membered ring amine.

Experimental Section

General Procedures. All experiments were conducted under inert atmosphere using a dual vacuum/nitrogen line and standard Schlenk techniques, being the corresponding workup carried out in air. ^{1}H and ^{13}C NMR spectra were recorded on a Bruker Avance-400 NMR spectrometer. Chemical shifts are reported relative to the residual solvent. Mass spectra (MS) were recorded on a VG Autospec Ultima MS spectrometer. All the solvents were purified prior to use. Toluene was purified over sodium/benzophenone ketyl, and distilled prior to use. Methanol was purified over anhydrous calcium chloride and distilled prior to use. 9,10-phenanthrenequinone (95%), 2,6-dimethylaniline (99%) and 2,6-diisopropylaniline (97%) were purchased from Aldrich and used as received.

General procedure for the syntheses of the monoimine compounds 1 and 2

A mixture of phenanthrenequinone (5.0 mmol) and substituted anilines (10.0 mmol) in methanol (50 ml), in the presence of formic acid (0.5 ml), was refluxed for 24 h. The solution was cooled down, concentrated to 30 ml by vacuum evaporation, and recrystallized at 0 ^{o}C. The products were finally isolated as deep blue crystals. Yields: 58 and 43%, respectively, for **1** and **2**.

Compound 1. ^{1}H NMR ($CDCl_3$, 400 MHz): δ 8.44 (d, *J*=7.6 Hz, 1H), 8.02 (br, 3H), 7.67 (t, *J*=7.2 Hz, 1H), 7.61 (t, *J*=7.2 Hz, 1H), 7.48 (t, *J*=7.6 Hz, 1H), 7.38 (t, *J*=7.2 Hz, 1H), 7.07 (d, *J*=7.6 Hz, 2H), 6.94 (t, *J*=7.6 Hz, 1H), 1.98 (s, 6H). ^{13}C NMR ($CDCl_3$, 75.46 MHz): δ 179.8, 153.9, 150.2, 136.7, 135.1, 132.6, 132.4, 132.2, 130.8, 129.5, 129.2, 128.7, 128.1, 127.6, 123.5, 123.4, 122.6, 122.5, 18.0. ESI-MS: m/z 311 $[M]^+$ (65%), 296 $[M\text{-}CH_3]^+$ (61%), 282 $[M\text{-}2CH_3\text{+}H]^+$ (100%). Anal. Calcd for $C_{22}H_{17}NO$: C, 84.86; H, 5.50; N, 4.50. Found: C, 84.69; H, 5.61; N, 4.42%.

Compound 2. ^{1}H NMR ($CDCl_3$, 400 MHz): δ 8.40 (d, *J*=7.2 Hz, 1H), 8.03 (d, *J*=8.0 Hz, 2H), 7.98 (d, *J*=8.0 Hz, 1H), 7.67 (t, *J*=8.4 Hz, 1H), 7.62 (t, *J*=7.6 Hz, 1H), 7.49 (t, *J*=7.2 Hz, 1H), 7.37 (t, *J*=7.2 Hz, 1H), 7.16 (d, *J*=6.8 Hz, 2H), 7.10 (t, *J*=6.8 Hz, 1H), 2.64 (m, 2H), 1.15 (d, *J*=6.8 Hz, 6H), 1.04 (d, *J*=6.4 Hz, 6H). ^{13}C NMR ($CDCl_3$, 75.46 Hz): δ 179.6, 153.9, 148.2,

136.6, 135.0, 132.9, 132.6, 132.4, 132.1, 131.4, 129.5, 129.3, 128.8, 128.3, 123.5, 123.4, 123.3, 122.8, 28.5, 23.0, 22.8. ESI-MS: m/z 367 $[M]^+$ (7%), 324 $[M\text{-}i\text{Pr}]^+$ (100%).

Synthesis of compound 3. Phenanthrenequinone (5.0 mmol), 2,6-diisopropylaniline (10.0 mmol), *p*-toluenesulfonic acid monohydrate (0.5 mmol) and toluene (50 ml) were added to a Schlenk flask equipped with a Dean-Stark trap. The mixture was refluxed for 24 h and the solvent was removed in vacuum (rotary evaporator). The bright yellow crystals were finally isolated after separation by elution through a silica-gel column using 1:10 ethyl acetate/hexane as eluent, and recrystallisation in heptane, at 0 ^oC. Yield: 42%. ^1H NMR ($CDCl_3$, 400 MHz): δ 7.92 (d, *J*=7.6 Hz, 1H), 7.86 (d, *J*=7.6 Hz, 1H), 7.82 (d, *J*=7.6 Hz, 1H), 7.66 (t, *J*=8.0 Hz, 1H), 7.54 (d, *J*=8.0 Hz, 1H), 7.39 (t, *J*=7.6 Hz, 1H), 7.34 (t, *J*=7.2 Hz, 1H), 7.23 (t, *J*=7.6 Hz, 1H), 7.10 (d, *J*=7.6 Hz, 1H), 6.84 (t, *J*=7.6 Hz, 1H), 6.72 (d, *J*=7.2 Hz, 1H), 4.69 (br, 1H), 3.17 (sept, *J*=7.2 Hz, 1H), 1.41 (d, *J*=6.4 Hz, 6H), 1.03 (s, 3H), 0.83 (s, 3H). ^{13}C NMR ($CDCl_3$, 75.46 Hz): δ 202.1, 146.2, 139.1, 138.0, 136.7, 134.4, 131.5, 131.3, 131.2, 128.7, 128.4, 128.0, 127.8, 126.9, 124.3, 124.0, 122.7, 120.8, 119.9, 79.9, 53.0, 29.0, 28.4, 24.9, 22.3, 22.1. ESI-MS: m/z 352 $[M\text{-}CH_3]^+$ (33%), 367 $[M]^+$ (100%).

X-Ray crystallography

Single crystals of **3** suitable for X-ray characterization were grown from a dilute heptane solution at 0 ^oC. Crystal data for compound **3** was collected in a Bruker AXS-KAPPA APEX II diffractometer equipped with an Oxford Cryosystem open-flow nitrogen cryostat, at 150 K, using graphite monochromated Mo-Kα radiation (λ=0.71073 Å). Cell parameters were retrieved using Bruker SMART software and refined using Bruker SAINT on all observed reflections. Absorption corrections were applied using SADABS.[13] Structure solution and refinement were performed using direct methods with the programs SIR2004[14] and SHELXL[15] both included in the package of programs WINGX-Version 1.70.01.[16] Non-hydrogen atoms were refined with anisotropic thermal parameters. Except H1n, that was found in the difference electron density map and was allowed to refine freely, all hydrogens were inserted in idealized positions and allowed to refine riding in the parent C atoms, with C-H distances of 0.93 Å, 0.96 Å and 0.98 Å for aromatic, methyl and methine H atoms respectively, and with *U*iso(H)=1.2*U*eq(C). For the isopropyl moiety, a certain extent of disorder is observed for atom C26, with 54% and 46% probability. All remaining crystal data and refinement parameters are presented in Table 3. Graphic presentations were prepared with ORTEP-III.[17]

CCDC-680335 contains the supplementary crystallographic data for this paper. These data can be obtained free of charge via www.ccdc.cam.ac.uk/data_request/cif, or by emailing data_request@ccdc.cam.ac.uk, or by contacting The Cambridge Crystallographic Data Centre, 12, Union Road, Cambridge CB2 1EZ, UK; fax: +44 1223 336033.

Computational details

All calculations were performed using the Gaussian 03 software package,[18] and the PBE1PBE functional, without symmetry constraints. That functional uses a hybrid generalized gradient approximation (GGA), including 25 % mixture of Hartree-Fock[19] exchange with DFT[7] exchange-correlation, given by Perdew, Burke and Ernzerhof functional (PBE).[20] The optimized geometries were obtained with a standard 6-31G(d,p)[21] basis set. Transition state optimizations were performed with the Synchronous Transit-Guided Quasi-Newton Method (STQN) developed by Schlegel *et al*.[22] Frequency calculations were performed to confirm the nature of the stationary points, yielding one imaginary frequency for the transition states and none for the minima. Each transition state was further confirmed by following its vibrational mode downhill on both sides, and obtaining the minima presented on the energy profile. Free energy values for the reaction profiles were obtained at 298.15 K and 1 atm by conversion of the zero point corrected electronic energies with the thermal energy corrections based on the calculated structural and vibrational frequency data. A Natural Population Analysis (NPA)[23] and the resulting Wiberg indices[12] were used to study the electronic structure and bonding of the optimized species.

Table 3. Crystal data and structure refinement for compound **3**

Empirical formula	$C_{26}H_{25}NO$
Formula weight	367.47
Temperature (K)	150(2)
Wavelength (Å)	0.71073
Crystal system	monoclinic
Space group	$P2_1/n$
Unit cell dimensions	a= 7.8021(7) Å α=90º
	b= 13.2580(9) Å β= 93.178(5)º
	c= 18.8037(17) Å γ=90º
V (Å^3)	1942.1(3)
Z	4
D_{calc} (Mg Å^{-3})	1.257
Absorption coefficient (mm^{-1})	0.076
F(000)	784
Crystal size (mm)	0.22×0.17×0.15
Theta range for data collection (º)	2.66-26.37
Index ranges	-9≤h≤9, -16≤k≤16, -23≤l≤23
Reflections collected	20712
Independent reflections	3984
Reflections observed [$I>2\sigma(I)$]	2500
R_{int}	0.1157
Refinement method	Full-matrix least-square on F^2

Table 3. Continued

Goodness-of-fit on F^2	1.007
R_1 [$I>2\sigma(I)$]	0.0601
wR_2 [$I>2\sigma(I)$]	0.1379
R_1, wR_2 all data	0.1044/ 0.1563
Largest difference peak and hole (e Å^{-3})	0.274/-0.268

Supporting Material Available

Figure containing the unit cell of the crystal structure of compound **3**. ^{1}H and ^{13}C{^{1}H} NMR spectra, and mass spectra of compounds **1**, **2** and **3**. Tables with atomic coordinates for all optimized species. CIF file of compound **3**.

Acknowledgements

We thank the Fundação para Ciência e Tecnologia for financial support (Projects PPCDT/QUI/59025/2004 and PTDC/QUI/65474/2006, co-financed by FEDER) and fellowships to L.L. and C.S.B.G. (SFRH/BPD/30733/2006 and SFRH/BD/16807/2004, respectively).

References and Notes

1. (a) Ittel, S. D.; Johnson, L. K. *Chem. Rev.* **2000**, *100*, 1169. (b) Britovsek, G. P.; Gibson, V. C.; Wass, D. F. *Angew. Chem. Int. Ed.* **1999**, *38*, 428. (c) Gibson, V. C.; Spitzmesser, S. K. *Chem. Rev.* **2003**, *103*, 283.
2. (a) Johnson, L. K.; Killian, C. M.; Brookhart, M. *J. Am. Chem. Soc.* **1995**, *117*, 6414. (b) Killian, C. M.; Tempel, D. J.; Johnson, L. K.; Brookhart, M. *J. Am. Chem. Soc.* **1996**, *118*, 11664. (c) Tempel, D. J.; Johnson, L. K.; Huff, R. L.; White, P. S.; Brookhart, M. *J. Am. Chem. Soc.* **2000**, *122*, 6686. (d) Gates, D. P.; Svejda, S. A.; Onate, E.; Killian, C. M.; Johnson, L. K.; White, P. S.; Brookhart, M. *Macromolecules* **2000**, *33*, 2320.
3. (a) Small, B. L.; Brookhart, M.; Bennett, A. M. *J. Am. Chem. Soc.* **1998**, *120*, 4049. (b) Britovsek, G. J. P.; Gibson, V. C.; Kimberley, B. S.; Maddox, P. J.; McTavish, S. J.; Solan, G. A.; White, A. J. P.; Williams, D. J. *Chem. Commun.* **1998**, 849.
4. (a) Pappalardo, D.; Mazzeo, M.; Antinucci, S.; Pellecchia, C. *Macromolecules* **2000**, *33*, 9483. (b) Guan, Z; B.; Cotts, M.; McCord, E. F.; McLain, S. J. *Science* **1999**, *283*, 2059. (c) Svejda, S. A.; Brookhart, M. *Organometallics* **1999**, *18*, 65. (d) Camacho, D. H.; Guan, Z. B. *Macromolecules*, **2005**, *38*, 2544. (e) Camacho, D. H.; Salo, E. V.; Ziller, J. W.; Guan, Z. B. *Angew. Chem. Int. Ed.* **2004**, *43*, 1821.

5. (a) Younkin, T. R.; Connor, E. F.; Henderson, J. I.; Friedrich, S. K.; Grubbs, R. H.; Bansleben, D. A. *Science* **2000**, *287*, 460. (b) Wang, C.; Friedrich, S.; Younkin, T. R.; Li, R. T.; Grubbs, R. H.; Bansleben, D. A.; Day, M. W. *Organometallics* **1998**, *17*, 3149. (c) Hicks, F. A.; Brookhart, M. *Organometallics* **2001**, *20*, 3217. (d) Zuideveld, M. A.; Wehrmann, P.; Rohr, C.; Mecking, S. *Angew. Chem. Int. Ed.* **2004**, *43*, 869. (e) Bauers, F. M.; Mecking, S. *Angew. Chem. Int. Ed.* **2001**, *40*, 3020. (f) Gottker-Schnetmann, I.; Korthals, B.; Mecking, S. *J. Am. Chem. Soc.* **2006**, *128*, 7708.
6. van Belzen, R.; Klein, R. A.; Smeets, W. J. J.; Spek, A. L.; Benedix, R.; Elsevier, C. J. *Recl. Trav. Chim. Pays-Bas* **1996**, *115*, 275.
7. Parr, R. G.; Yang W. *Density Functional Theory of Atoms and Molecules*, Oxford University Press: New York, 1989.
8. (a) Layer, R. W. *Chem. Rev.* **1963**, *63*, 489. (b) Sprung, M. M. *Chem. Rev.* **1940**, *26*, 297.
9. Abakumov, G. A.; Cherkasov, V. K.; Druzhkov, N. O.; Kurskii, Y. A.; Fukin, G. K.; Abakumova, L. G.; Kocherova, T. N. *Synth. Commun.* **2006**, *36*, 3241.
10. (a) Cho, B. T.; Kang, S. K. *Tetrahedron* **2005**, *61*, 5725. (b) Sato, S.; Sakamoto, T.; Miyazawa, E.; Kikugawa, Y. *Tetrahedron* **2004**, *60*, 7899. (c) Apodaca, R.; Xiao, W. *Org. Lett.* **2001**, *3*, 1745. (d) Abdel-Magid, A. F.; Mayano, C. A.; Carson, K. G. *Tetrahedron Lett.* **1990**, *31*, 5595.
11. (a) Kitamura, M.; Lee, D. H.; Hayashi, S.; Tanaka, S.; and Yoshimura, M. *J. Org. Chem.* **2002**, *67*, 8685. (b) Kadyrov, R.; Riermeier, T. H. *Angew. Chem. Int. Ed.* **2003**, *42*, 5472.
12. (a) Wiberg, K. B. *Tetrahedron* **1968**, *24*, 1083. (b) Wiberg indices are electronic parameters related to the electron density between atoms. They can be obtained from a Natural Population Analysis and provide an indication of the bond strength.
13. Sheldrick, G. M. *SADABS, Program for Empirical Absorption Correction*, University of Göttingen, Göttingen, 1996.
14. Burla, M. C.; Caliandro, R.; Camalli, M.; Carrozzini, B.; Cascarano, G. L.; De Caro, L.; Giacovazzo, C.; Polidori, G.; Spagna, R. *J. Appl. Cryst.* **2005**, *38*, 381.
15. Sheldrick, G. M. *Shelxl-97-A Computer Program for Refinement of Crystal Structure*, University of Göttigen, Göttigen, 1997.
16. Farrugia, L. J. *J. Appl. Cryst.* **1999**, *32*, 837.
17. Burnett, M. N.; Johnson, C. K. *ORTEP-III: Oak Ridge Thermal Ellipsoid Plot Program for Crystal Structure Illustration*, Oak Ridge National Laboratory Report ORNL-6895, 1996.
18. Frisch, M. J.; Trucks, G. W.; Schlegel, H. B.; Scuseria, G. E.; Robb, M. A.; Cheeseman, J. R.; Montgomery, Jr., J. A.; Vreven, T.; Kudin, K. N.; Burant, J. C.; Millam, J. M.; Iyengar, S. S.; Tomasi, J.; Barone, V.; Mennucci, B.; Cossi, M.; Scalmani, G.; Rega, N.; Petersson, G. A.; Nakatsuji, H.; Hada, M.; Ehara, M.; Toyota, K.; Fukuda, R.; Hasegawa, J.; Ishida, M.; Nakajima, T.; Honda, Y.; Kitao, O.; Nakai, H.; Klene, M.; Li, X.; Knox, J. E.; Hratchian, H. P.; Cross, J. B.; Adamo, C.; Jaramillo, J.; Gomperts, R.; Stratmann, R. E.; Yazyev, O.; Austin, A. J.; Cammi, R.; Pomelli, C.; Ochterski, J. W.; Ayala, P. Y.; Morokuma, K.; Voth, G. A.; Salvador, P.; Dannenberg, J. J.; Zakrzewski, V. G.; Dapprich, S.; Daniels, A. D.;

Strain, M. C.; Farkas, O.; Malick, D. K.; Rabuck, A. D.; Raghavachari, K.; Foresman, J. B.; Ortiz, J. V.; Cui, Q.; Baboul, A. G.; Clifford, S.; Cioslowski, J.; Stefanov, B. B.; Liu, G.; Liashenko, A.; Piskorz, P.; Komaromi, I.; Martin, R. L.; Fox, D. J.; Keith, T.; Al-Laham, M. A.; Peng, C. Y.; Nanayakkara, A.; Challacombe, M.; Gill, P. M. W.; Johnson, B.; Chen, W.; Wong, M. W.; Gonzalez, C. and Pople, J. A. *GAUSSIAN 03*, Revision C.02, Gaussian Inc.: Wallingford CT, 2004.

19. Hehre, W. J.; Radom, L.; Schleyer, P. v. R.; Pople, J. A. *Ab Initio Molecular Orbital Theory*, John Wiley & Sons: New York, 1986.
20. (a) Perdew, J. P.; Burke, K.; Ernzerhof, M. *Phys. Rev. Lett.* **1997**, *78*, 1396. (b) Perdew, J. P. *Phys. Rev. B* **1986**, *33*, 8822.
21. (a) Ditchfield, R.; Hehre, W. J.; Pople, J. A. *J. Chem. Phys.* **1971**, *54*, 724. (b) Hehre, W. J.; Ditchfield, R.; Pople, J. A. *J. Chem. Phys.* **1972**, *56*, 2257. (c) Hariharan, P. C.; Pople, J. A. *Mol. Phys.* **1974**, *27*, 209. (d) Gordon, M. S. *Chem. Phys. Lett.* **1980**, *76*, 163. (e) Hariharan, P. C.; Pople, J. A. *Theor. Chim. Acta* **1973**, *28*, 213.
22. (a) Peng, C. Y.; Ayala, P. Y.; Schlegel, H. B.; Frisch, M. J. *J. Comp. Chem.* **1996**, *17*, 49. (b) Peng, C.; Schlegel, H. B. *Israel J. Chem.* **1993**, *33*, 449.
23. (a) Carpenter, J. E.; Weinhold, F. *J. Mol. Struct. (Theochem)* **1988**, *169*, 41. (b) Carpenter, J. E. PhD thesis, University of Wisconsin (Madison WI), 1987. (c) Foster, J. P.; Weinhold, F. *J. Am. Chem. Soc.* **1980**, *102*, 7211. (d) Reed, A. E.; Weinhold, F. *J. Chem. Phys.* **1983**, *78*, 4066. (e) Reed, A. E.; Weinhold, F. *J. Chem. Phys.* **1985**, *78*, 1736. (f) Reed, A. E.; Weinstock, R. B.; Weinhold, F. *J. Chem. Phys.* **1985**, *83*, 735. (g) Reed, A. E.; Curtiss, L. A.; Weinhold, F. *Chem. Rev.* **1988**, *88*, 899. (h) Weinhold, F.; Carpenter, J. E. in *The Structure of Small Molecules and Ions*, Plenum: New York, 1988; p. 227.